

AD-A043 356

WEIDLINGER ASSOCIATES NEW YORK

F/G 20/4

ON UNCOUPLING STRUCTURE-FLUID INTERACTION PROBLEMS STATUS REPORT--ETC(U)

MAY 77 H H BLEICH, F L DIMAGGIO, D RANLET

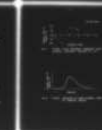
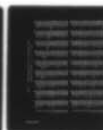
N00014-72-C-0119

NL

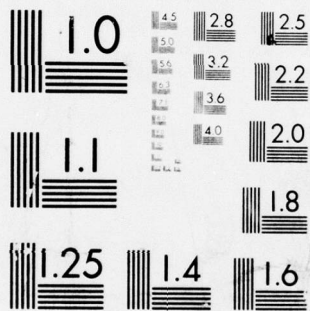
UNCLASSIFIED

| OF |
AD
A043 356

1



END
DATE
FILMED
9-77
DDC



MICROCOPY RESOLUTION TEST CHART
NATIONAL BUREAU OF STANDARDS-1963-A

AD A 043356

WEIDLINGER ASSOCIATES

110 EAST 59TH STREET

NEW YORK, NEW YORK 10022

6
B.S.

ON UNCOUPLING STRUCTURE-FLUID INTERACTION PROBLEMS
STATUS REPORT ON THE IDCA

by

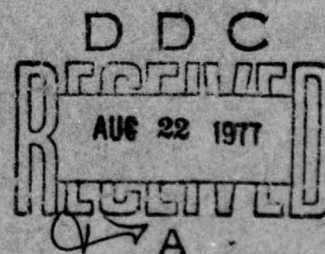
H. H. Bleich, F. L. DiMaggio, D. Ranlet and M. L. Baron

OFFICE OF NAVAL RESEARCH

CONTRACT N00014-72-C-0119

TECHNICAL NOTE

MAY 1977



This project is sponsored by the joint DNA/ONR/NAVSEA program in
"Advanced Submarine Shock Survivability in Underwater Nuclear Attack."

Approved for public release; Distribution unlimited.

AD NO.
DDC FILE COPY

6

6

ON UNCOUPLING STRUCTURE-FLUID INTERACTION PROBLEMS

STATUS REPORT ON THE IDCA

by

10

H.H. Bleich, F.L. DiMaggio, D. Ranlet and M.L. Baron

15

OFFICE OF NAVAL RESEARCH

CONTRACT N00014-72-C-0119

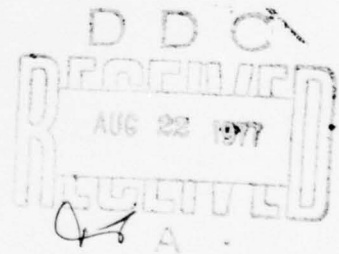
9

TECHNICAL NOTE

11

May 1977

12 23p.



This project is sponsored by the joint DNA/ONR/NAVSEA program in "Advanced Submarine Shock Survivability in Underwater Nuclear Attack".

Approved for public release; Distribution unlimited.

373 050

mt

TABLE OF CONTENTS

	<u>Page</u>
I. INTRODUCTION	1
II. DESCRIPTION OF THE INERTIAL-DAMPING COLLOCATION APPROXIMATION. .	2
III. DIFFICULTIES ENCOUNTERED	5
IV. IMPROVED FITTING PROCEDURE	7
REFERENCES	10
TABLES	11
FIGURES.	13
APPENDIX	17

ACCESSION FOR	
NTIS	White Section <input checked="" type="checkbox"/>
DTIC	Gen Section <input type="checkbox"/>
UNANNOUNCED	<input type="checkbox"/>
CLASSIFICATION	
DISTRIBUTION AVAILABILITY CODES	
DOWNTON	
REEL, END, OR SPECIAL	
A	

I. INTRODUCTION

In the last few years, a concerted effort has been made to analyze submerged structures under explosive loadings, by utilizing the Doubly Asymptotic Approximation (DAA), Ref. [1], to account for the structure-fluid interaction. The current implementation of the DAA, by Weidlinger Associates, Ref. [2] to [5], employs a modal analysis for the structure and a set of orthogonal functions (surface expansion functions) for the fluid, the latter being used to improve the conditioning of the governing response equations.

The DAA yields exact results for high and low frequencies and produces a smooth transition between these limits. Since a more accurate fit at intermediate frequencies may prove to be important in some problems of interest, the DAA may prove to be inadequate in some cases. Thus, work was done on developing improvements to the DAA. One such approach, the Inertial-Damping Collocation Approximation (IDCA), was developed by Weidlinger Associates several years ago and was reported on in Ref. [2]. The IDCA gives exact results for low, high, and selected intermediate frequencies, and as such represents a potential improvement over the DAA.

Although the IDCA was described in Ref. [2], problems arising from the fitting procedures used to match exact steady-state results were not discussed in detail. With some current interest in the development of improved uncoupling techniques, this note has been prepared to document the current status of the IDCA and to demonstrate the new improved fitting procedures developed for the application of this method.

II. DESCRIPTION OF THE INERTIAL-DAMPING COLLOCATION APPROXIMATION

For a submerged structure subjected to an underwater explosion, it is possible to approximate the structure-fluid interaction by expressing the surface pressures in terms of the normal surface velocities (Refs. [1] and [2]). Such a procedure essentially uncouples the fluid from the structure by subjecting the structure in-vacuo to free-field effects plus a structure-fluid interaction loading. The DAA, for example, is an uncoupling technique which yields correct results for low and high frequencies. In this section, a new uncoupling scheme, the IDCA, will be described briefly. This method allows matching exact solutions for low, high, and selected intermediate frequencies.

Let a time-harmonic normal displacement be applied to a fluid surface (cavity) having the shape of a structure to be submerged and loaded by an underwater explosion:

$$w(s, t) = W(s) e^{i\Omega t} \quad (1)$$

where s denotes position on the surface, t represents time, and $i = \sqrt{-1}$. The radiated fluid pressure may then be written in the form

$$p(s, t) = [\bar{p}(s) + i \bar{\bar{p}}(s)] e^{i\Omega t} \quad (2)$$

in which the inertial (real) component, \bar{p} , is in phase with the displacement, and the damping (imaginary) component, $\bar{\bar{p}}$, is in phase with the velocity.

For arbitrary excitation of a submerged structure, the radiated pressure (the difference between the total and incident pressures on the surface of the structure) may also be represented by a component in phase with the displacement of the surface of the structure and a component in

phase with the normal velocity of the surface. The generalized force associated with the radiated pressure may then be expressed as

$$\hat{\underline{Q}} = \hat{\underline{Q}}_1 + \hat{\underline{Q}}_2 \quad (3)$$

where $\hat{\underline{Q}}_1$ and $\hat{\underline{Q}}_2$ have the characters of an inertia force and a damping force, respectively, underlining denotes a matrix, and the caps indicate a formulation of the fluid response based on surface expansion functions rather than structural modes.

When based on surface expansion functions, the IDCA may be written as^{*)}

$$\hat{\underline{q}} - \int_0^t \hat{\underline{U}}_I dt - \underline{a}(\hat{\underline{q}} - \hat{\underline{U}}_I) = \hat{\underline{\gamma}}^{-1} \int_0^t \int_0^t \hat{\underline{Q}}_1 dt dt + \underline{B} \hat{\underline{Q}}_1 + \underline{C} \hat{\underline{Q}}_1 \quad (4)$$

$$\hat{\underline{q}} - \hat{\underline{U}}_I = \underline{D} \int_0^t \hat{\underline{Q}}_2 dt - \hat{\underline{\alpha}}^{-1} \hat{\underline{Q}}_2 \quad (5)$$

in which $\hat{\underline{q}}$ is the array of generalized coordinates for the fluid, $\hat{\underline{U}}_I$ is the array of expansion coefficients for the incident (free-field) velocity, $\hat{\underline{\gamma}}$ is the virtual mass matrix, $\hat{\underline{\alpha}}$ is the diagonal radiation damping matrix, and a dot indicates differentiation with respect to time. The elements of matrices \underline{B} , \underline{C} , \underline{D} are evaluated by matching exact steady-state solutions at selected frequencies.

For low frequencies, Eq. (4) reduces to the Virtual Mass Approximation (Ref. [6]), and for high frequencies, Eq. (5) reduces to the Plane Wave Approximation (Ref. [7]). The matrix \underline{a} in Eq. (4) is used to ensure the

*) If a submerged body is subjected to an incident pressure wave with zero rise time, a time-integrated form of Eqs. (4) and (5) should be used, as shown in Ref. [2].

correct asymptotic behavior of the inertial part of the IDCA for high frequencies (Curved Wave Approximation, Ref. [8]). Details of the procedures used to obtain the elements of \underline{a} , \underline{B} , \underline{C} , \underline{D} may be found in Ref. [2].

III. DIFFICULTIES ENCOUNTERED

In the IDCA, fitting is employed for the relations between normal surface displacements and the resulting generalized forces considered as functions of the frequency. The concept of fitting was developed after a study of simple cases (infinitely long cylindrical and spherical shells) where one displacement mode and one force are fitted at a time. In this situation the fitted curves are necessarily smooth, and in general acceptable. In the general case, a considerable number of surface expansion coordinates and the corresponding forces are fitted simultaneously, and the success of this fitting process was a major matter of concern for the investigators.

Discussing as a typical example the case $N = 1$ (one circumferential wave) for the structure treated in Ref. [3] (ring-stiffened circular cylindrical shell closed by flat end plates), it was found that the fitting process properly reproduced the desired values of the fluid resistance^{*)} at the frequencies selected for fitting. However, the curves were not as smooth as hoped. While the oscillations in most cases are minor, there are a number of cases with violent oscillations in narrow frequency ranges. In the case under discussion, 18 surface expansion functions and the corresponding 18 generalized forces were used, and the resulting relations plotted. In two cases the values $\hat{\gamma}_R$ (accession to mass) oscillated so severely that the values became negative for a narrow frequency range. Figures 1 to 4 show as

^{*)} In this note, the term fluid resistance is used to denote the array $\gamma = \hat{\gamma}_R + i \hat{\gamma}_I$, in which $\hat{\gamma}_R$ and $\hat{\gamma}_I$ have real elements and $i = \sqrt{-1}$. The array $\hat{\gamma}_R$ has the character of the specific acoustic inertia, while $\Omega \hat{\gamma}_I$, where Ω represents frequency, has the character of the specific acoustic resistance. The exact frequency dependence of γ was obtained by modifying an existing sound radiation code (Ref. [9]).

examples plots of $\hat{\gamma}_R$ for surface expansion functions 1, 2, 5 and 12. For function 1, the rigid body displacement, $\hat{\gamma}_R$ is in general well approximated, but there are slight oscillations below $f = 0.5$ kcps. For functions 2 and 12, Figs. 2 and 4 show the worst situations encountered; they give unrealistic negative values for $\hat{\gamma}_R$ at certain frequencies. An intermediate situation for function 5 is shown in Fig. 3. There are strong oscillations, but no negative values for $\hat{\gamma}_R$. The fitting of the values $\hat{\gamma}_I$ (damping) does not lead to violent oscillations as was the case in Figs. 2 to 4. The result for the rigid body motion, function 1, is shown in Fig. 5. However, inspection of the results for the remainder of the surface expansion functions disclosed two cases, functions 12 and 13, shown in Figs. 6 and 7, where the damping $\hat{\gamma}_I$ becomes negative for frequencies below $f \sim 1.5$ kcps.

It would be legitimate to reason that local oscillations in the curves for $\hat{\gamma}_R$ and $\hat{\gamma}_I$ should not cause unrealistic final results, because the response is inherently a composite of effects originating from all frequencies. However, the occurrence of regions of negative damping or negative accession to mass makes the results of the analysis tainted, although only 4 of the total of 18 relations are thus affected. Thought was therefore given to variations of the scheme which avoided the described undesirable situations.

IV. IMPROVED FITTING PROCEDURE

If the IDCA in terms of surface expansion functions, as described in Ref. [2], is applied to an infinitely long cylindrical shell (or to a spherical one) of uniform thickness, the difficulties described in Section III could not occur, because only one surface expansion coordinate and one generalized force couple. This simple situation is caused by the fact that the matrices $\hat{\gamma}_R$ and $\hat{\gamma}_I$ are diagonal. This suggests that one could avoid these difficulties if one could select surface expansion functions such that the matrices $\hat{\gamma}_R$ and $\hat{\gamma}_I$ are diagonal at all frequencies. This ideal solution is not available for a general, complex structure.

However, one can start by selecting surface expansion functions $\hat{\psi}_j(s)$ which make the matrices $\hat{\gamma}_R$ and $\hat{\gamma}_I$ diagonal for $\Omega = 0$ and $\Omega \rightarrow \infty$, respectively, where Ω denotes frequency. This is always possible, and can be done as described in the Appendix. (Note that the previously proposed functions $\psi_j(s)$ already lead to a diagonal matrix $\hat{\gamma}_I$ for $\Omega \rightarrow \infty$.) At intermediate frequencies, such as those selected for fitting, the matrices $\hat{\gamma}_R$ and $\hat{\gamma}_I$ would not be diagonal. However, since $\hat{\gamma}_R$ and $\hat{\gamma}_I$ are diagonal for $\Omega = 0$ and $\Omega \rightarrow \infty$, respectively, one may expect that the matrices at intermediate frequencies are sufficiently close to diagonal to permit ignoring, as an approximation, the off-diagonal terms. Such an approach leads to an IDCA-solution without problems caused by negative accession to mass or negative damping.

In order to evaluate this idea, a unique, but of course truncated set of surface expansion functions was obtained, such that the matrices $\hat{\gamma}_R$ and $\hat{\gamma}_I$ were diagonal for $\Omega = 0$ and $\Omega \rightarrow \infty$, respectively. This was again done for the case studied in Section III. Using these new surface expansion functions, the matrices $\hat{\gamma}_R$ and $\hat{\gamma}_I$ were computed at several intermediate

frequencies to verify the order of magnitude of the off-diagonal terms to be ignored.

In the earlier scheme using the complete matrix of the fluid resistance, including the off-diagonal terms, certain fitting frequencies were selected. Obviously, the importance of the off-diagonal terms to be dropped in the newly proposed scheme should be considered at the level of the fitting frequencies appropriate for the new scheme. The frequency dependence of the fluid resistance in either scheme depends on the typical distance between the nodal lines of the imposed displacements, i.e., the surface expansion functions. This may be seen, typically, for the scheme for which fitting results are shown in Figs. 1 to 7. The values $\hat{\gamma}_R$ (accession to mass) were fitted for one frequency above and one frequency below the peak of a curve. The peak shifts to higher frequencies as the mode number increases, because the nodal distances decrease with mode number. The peak is located at quite a low frequency ($f \sim 0.3$ kcps) for function 1, higher frequency ($f \sim 1$ kcps) for function 5, and much higher frequency for function 12. A shift of fitting frequencies through the same range is to be expected for the proposed new surface expansion functions. The range $f = 0.5$ to 2.5 kcps was therefore studied carefully.

The method shown in the Appendix was applied to determine the fluid resistance ($\hat{\gamma}_R$ and $\hat{\gamma}_I$) based on transformed surface expansion functions $\hat{\psi}_j(s)$. Little difference in the importance of the off-diagonal terms in $\hat{\gamma}_R$ (accession to mass) was observed over the above range of frequencies. As typical, Table I shows the matrix for $f = 1$ kcps. Inspection of the Table indicates that the off-diagonal terms are nearly always less, often very much less, than $1/10$ of the diagonal ones. The ignoring of such small terms seems reasonable.

The check on the importance of the off-diagonal terms for the matrix $\hat{\gamma}_I$ (damping) is slightly more complex because of the nature of these curves. They have the character of Fig. 8. The values are practically zero from $f = 0$ to some value close to the fitting point, $\bar{\Omega}$. As a result, the prevailing of the diagonal terms is of importance only near the fitting frequency for the respective function. At frequencies below the fitting point, the diagonal and the off-diagonal terms are several orders of magnitude smaller than near the fitting point. The situation away from fitting points is thus of no consequence. This is illustrated in Tables II to IV. For the first five transformed functions $\hat{\psi}_j$ the fitting points are below or up to $f = 1$ kcps, and Table II shows the matrix $\hat{\gamma}_I$ for the lowest values $k, j \leq 5$. The diagonal terms prevail, not so strongly as for $\hat{\gamma}_R$, but still with factors close to 10. On the other hand, for the same frequency the diagonal terms do not prevail for higher functions, as may be seen from Table III for $k, j = 12$ to 18. However, the values $\hat{\gamma}_I$ are here of the order 10^{-2} and 10^{-3} , i.e., extremely small compared to the diagonal terms in Table II, which are of the order 10^{+1} . For values $k, j \geq 12$ the fitting frequencies are in the $f = 3$ to 4 kcps range, and Table IV shows the appropriate portion of the matrix $\hat{\gamma}_I$. It is seen that the diagonal terms in this range prevail strongly, with factors larger than 10.

It is thus concluded that the proposal to disregard off-diagonal terms^{*)} appears to be a promising approximation.

*) It is noted that an entirely different fitting scheme, involving the use of convolution integrals was suggested at a technical meeting at DNA in July 1974 by Dr. T. Geers. The scheme was based on surface expansion functions which lead to diagonalized matrices γ_R and γ_I at $\Omega = 0$ and $\Omega \rightarrow \infty$, respectively. This scheme also ignored off-diagonal terms at intermediate frequencies. The degree of approximation obtainable by any such scheme, shown here in Tables I to IV, has however not been demonstrated previously.

REFERENCES

- [1] T.L. Geers, "Residual Potential and Approximate Methods for Three-Dimensional Fluid-Structure Interaction Problems", Journal of the Acoustical Society of America, Vol. 49, No. 5 (Part 2), 1971, pp. 1505-1510.
- [2] H.H. Bleich, F.L. DiMaggio, M.L. Baron and D. Ranlet, "Transient Response of Submerged Shells of Finite Length to Full Envelopment Type Shock Waves, Part I: Acoustic Approximations for Uncoupling Fluid-Structure Interaction Problems", Technical Report No. 13, Weidlinger Associates, New York, New York, Office of Naval Research, Contract No. N00014-72-C-0119, July 1974.
- [3] D. Ranlet, F.L. DiMaggio, H.H. Bleich and M.L. Baron, "An Improvement in the Use of the Doubly Asymptotic Approximation in Predicting the Transient Response of Submerged Shells of Finite Length to Full-Envelopment Shock Waves (U)", Technical Report No. 18, Confidential, Weidlinger Associates, New York, New York, Office of Naval Research, Contract No. N00014-72-C-0119, February 1975.
- [4] D. Ranlet, H.H. Bleich, F.L. DiMaggio and M.L. Baron, "Transient Response of Submerged Shells of Finite Length to Full Envelopment Type Shock Waves, Part IV: Comparison of Predicted and Measured Results for Side-On Loading of a Shell Containing Internal Structure - Configuration 1", Technical Report No. 17, Weidlinger Associates, New York, New York, Office of Naval Research, Contract No. N00014-72-C-0119, December 1974.
- [5] D. Ranlet, H.H. Bleich, F.L. DiMaggio and M.L. Baron, "Transient Response of Submerged Shells of Finite Length to Full Envelopment Type Shock Waves, Part V: Comparison of Predicted and Measured Results for Side-On Loading of a Shell Containing Internal Structure - Configuration 3 (U)", Technical Report No. 19, Weidlinger Associates, New York, New York, Office of Naval Research, Contract No. N00014-72-C-0119, August 1975.
- [6] G. Chertock, "Transient Flexural Vibrations of Ship-Like Structures Exposed to Underwater Explosions", Journal of the Acoustical Society of America, Vol. 48, No. 1 (Part 2), 1970, pp. 170-180.
- [7] R.D. Mindlin and H.H. Bleich, "Response of an Elastic Cylindrical Shell to a Transverse, Step Shock Wave", Journal of Applied Mechanics, 20 (1953), p. 189.
- [8] B. Bedrosian and F.L. DiMaggio, "Acoustic Approximations in Fluid-Shell Interactions", Journal of Engineering Mechanics Division, A.S.C.E., June 1972, p. 731.
- [9] J.M. McCormick, M.L. Baron and D. Ranlet, "Sound Radiation from Submerged Stiffened Cylindrical Shells of Finite Length with Flexible End Caps", Technical Report No. 9, Weidlinger Associates, New York, New York, Office of Naval Research, Contract No. N00014-70-C-0359, August 1970.

TABLE I. INERTIA MATRIX $\hat{\gamma}_R$ BASED ON TRANSFORMED SURFACE EXPANSION FUNCTIONS -- $N = 1$, $f = 1$ KCPS

1	-9.0284	1	-9.0284	2	-0.1532	3	-0.2175	4	-0.2812	5	0.1020	6	0.1398	7	0.0121	8	-0.0752	9	-0.0975
2	-0.1533	-10.3690	-0.4786	-0.5958	0.4688	0.4313	0.524	0.1921	-0.2513					0.0524	0.1921			-0.2513	
3	-0.2193	-0.4824	-13.8893	-0.7835	1.2504	0.9186	0.1750	-0.2817	-0.3929					0.1750	-0.2817			-0.3929	
4	-0.2896	-0.6152	-0.8043	-23.5086	3.7214	2.1225	0.6294	-0.2375	-0.4744					0.6294	-0.2375			-0.4744	
5	0.0765	0.4085	1.1648	3.6304	-37.6869	1.8929	0.9589	0.4276	0.2011					0.9589	0.4276			0.2011	
6	0.1381	0.4265	0.9077	2.1142	1.9582	-25.0924	-0.1023	-0.0781	-0.0249					-0.1023	-0.0781			-0.0249	
7	0.0269	0.0862	0.2197	0.6928	1.1275	0.0109	-19.9279	-0.1246	-0.0723					-19.9279	-0.1246			-0.0723	
8	-0.0551	-0.1455	-0.2172	-0.1502	0.6107	0.0767	-0.0462	-16.6449	-0.0535					-0.0462	-16.6449			-0.0535	
9	-0.0791	-0.2088	-0.3336	-0.3964	0.3504	0.1178	0.0274	-0.0159	-14.2015					0.0274	-0.0159			-14.2015	
10	-0.0805	-0.2098	-0.3358	-0.4274	0.2345	0.1342	0.0665	0.0169	-0.0033					0.0665	0.0169			-0.0033	
11	-0.0766	-0.1975	-0.3151	-0.4119	0.1713	0.1390	0.0874	0.0368	0.0108					0.0874	0.0368			0.0108	
12	0.0720	0.1841	0.2933	0.3919	-0.1250	-0.1373	-0.0989	-0.0502	-0.0215					-0.0989	-0.0502			-0.0215	
13	0.0665	0.1690	0.2704	0.3720	-0.0792	-0.1298	-0.1050	-0.0608	-0.0313					-0.1050	-0.0608			-0.0313	
14	0.0568	0.1440	0.2332	0.3354	-0.0235	-0.1106	-0.1032	-0.0686	-0.0414					-0.1032	-0.0686			-0.0414	
15	0.0395	0.1003	0.1666	0.2577	0.0379	-0.0723	-0.0845	-0.0665	-0.0469					-0.0845	-0.0665			-0.0469	
16	0.0189	0.0482	0.0856	0.1533	0.0824	-0.0245	-0.0503	-0.0505	-0.0419					-0.0503	-0.0505			-0.0419	
17	0.0033	0.0092	0.0238	0.0676	0.0992	0.0117	-0.0188	-0.0313	-0.0317					-0.0188	-0.0313			-0.0317	
18	0.0361	0.0869	0.1092	0.0489	-0.3473	-0.1616	-0.0603	0.0198	0.0538					-0.0603	0.0198			0.0538	
1	-0.0960	10	11	12	13	14	15	16	17	18									
2	-0.2457	-0.0896	0.0831	0.0759	0.0647	0.0423	0.0423	0.0181	0.0004	0.0509									
3	-0.3858	-0.2277	0.2100	0.1912	0.1631	0.1076	0.1076	0.0473	0.0031	0.1190									
4	-0.4907	-0.4611	0.3284	0.2995	0.2575	0.1728	0.1728	0.0802	0.0116	0.1638									
5	0.1228	0.0956	0.4295	0.3973	0.3500	0.2421	0.2421	0.1226	0.0312	0.1713									
6	0.0153	0.0459	-0.0851	-0.0842	-0.0838	-0.0998	-0.0998	-0.0853	-0.0664	0.1374									
7	-0.0309	0.0002	-0.0714	-0.1003	-0.1333	-0.1644	-0.1644	-0.1530	-0.1244	0.2711									
8	-0.0339	0.0180	-0.0251	-0.0522	-0.0862	-0.1204	-0.1204	-0.1211	-0.1044	0.2488									
9	-0.0213	-0.0172	0.0053	-0.0083	-0.0280	-0.0501	-0.0501	-0.0564	-0.0524	0.1378									
10	-12.3822	-0.1119	0.0141	0.0108	0.0033	-0.0076	-0.0076	-0.0142	-0.0163	0.0528									
11	-0.0002	-0.0919	0.0140	0.0165	0.0161	0.0120	0.0120	0.0067	0.0024	0.0051									
12	-0.0078	0.0004	0.0113	0.0173	0.0212	0.0214	0.0214	0.0175	0.0127	-0.0237									
13	-0.0159	-0.0059	-0.8949	-0.0164	-0.0231	-0.0263	-0.0263	-0.0240	-0.0195	0.0450									
14	-0.0258	-0.0154	-0.0032	-9.0188	-0.0220	-0.0281	-0.0281	-0.0283	-0.0249	0.0652									
15	-0.0343	-0.0255	0.0059	-0.0045	-8.3260	-0.0244	-0.0244	-0.0283	-0.0276	0.0816									
16	-0.0347	-0.0293	0.0177	0.0087	-0.0018	-7.7669	-7.7669	-0.0215	-0.0243	0.0828									
17	-0.0294	-0.0272	0.0244	0.0183	0.0097	-0.0016	-0.0016	-7.2674	-0.0163	0.0665									
18	0.0658	0.0716	0.0251	0.0218	0.0160	0.0071	0.0071	-0.0020	-6.7989	0.0438									
			-0.0754	-0.0769	-0.0717	-0.0556	-0.0556	-0.0315	-0.0107	-5.8885									

TABLE II. DAMPING MATRIX $\hat{\gamma}_I$ FOR TRANSFORMED SURFACE
EXPANSION FUNCTIONS 1 TO 5 -- N = 1, f = 1 KCPS

	1	2	3	4	5
1	24.8457	-.0387	-.1005	-.2540	-.5858
2	-.0383	25.7018	-.3079	-.7088	-1.4447
3	-.0997	-.3073	27.7117	-1.3312	-2.4059
4	-.2537	-.7092	-1.3318	30.0487	-3.9177
5	-.6139	-1.5114	-2.4974	-4.0240	13.2663

TABLE III. DAMPING MATRIX $\hat{\gamma}_I$ FOR TRANSFORMED SURFACE
EXPANSION FUNCTIONS 12 TO 18 -- N = 1, f = 1 KCPS

	12	13	14	15	16	17	18
12	.0188	.0424	.0378	.0336	.0232	.0137	-.0095
13	.0388	.0262	.0359	.0317	.0226	.0135	-.0105
14	.0317	.0325	.0403	.0259	.0192	.0116	-.0092
15	.0227	.0235	.0216	.0306	.0155	.0094	-.0081
16	.0123	.0132	.0127	.0121	.0127	.0054	-.0052
17	.0038	.0044	.0044	.0043	.0034	.0014	-.0029
18	.0167	.0160	.0149	.0127	.0077	.0037	-.0022

TABLE IV. DAMPING MATRIX $\hat{\gamma}_I$ FOR TRANSFORMED SURFACE
EXPANSION FUNCTIONS 12 TO 18 -- N = 1, f = 4 KCPS

	12	13	14	15	16	17	18
12	8.1935	.1076	.1297	.1289	.0836	.1249	-.7472
13	.0953	8.5436	.1493	.1457	.0665	.1576	-.7384
14	.1063	.1387	9.1479	.1569	.0202	.2057	-.5789
15	.1032	.1338	.1578	10.1006	-.0780	.2416	-.1254
16	.0792	.0969	.1020	.0522	11.4324	.2216	.6129
17	.0854	.1001	.1069	.0691	-.1346	13.9239	1.4480
18	-.6427	-.6361	-.4815	-.0299	.7313	1.4785	11.1495

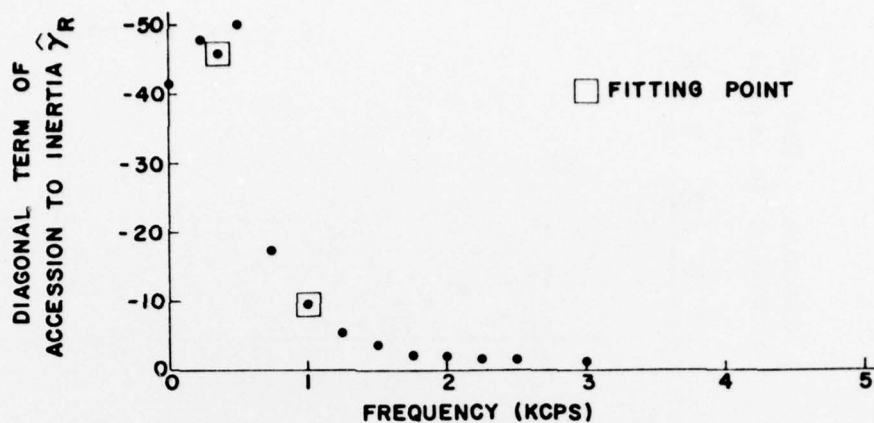


FIG. 1 FITTED FLUID RESPONSE (REAL PART)
SURFACE EXPANSION FUNCTION 1, N=1

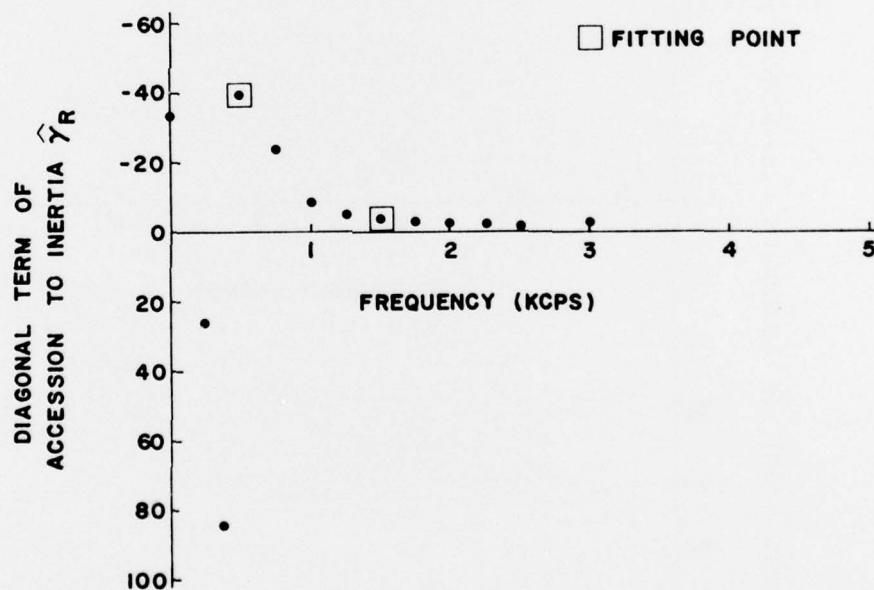


FIG. 2 FITTED FLUID RESPONSE (REAL PART)
SURFACE EXPANSION FUNCTION 2, N=1

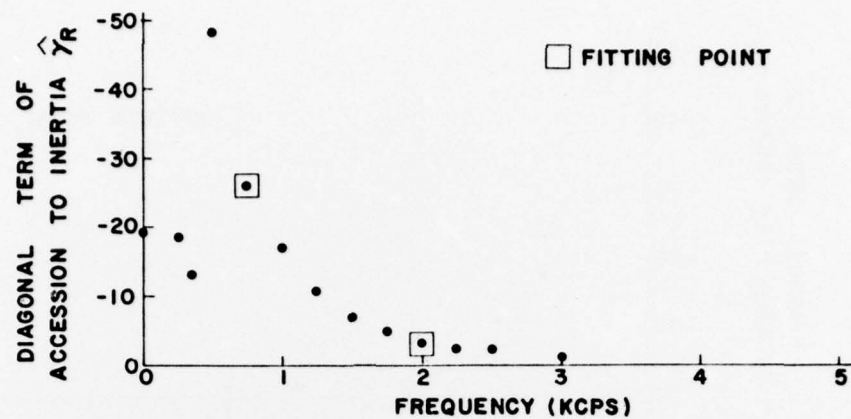


FIG. 3 FITTED FLUID RESPONSE (REAL PART)
SURFACE EXPANSION FUNCTION 5, N=1

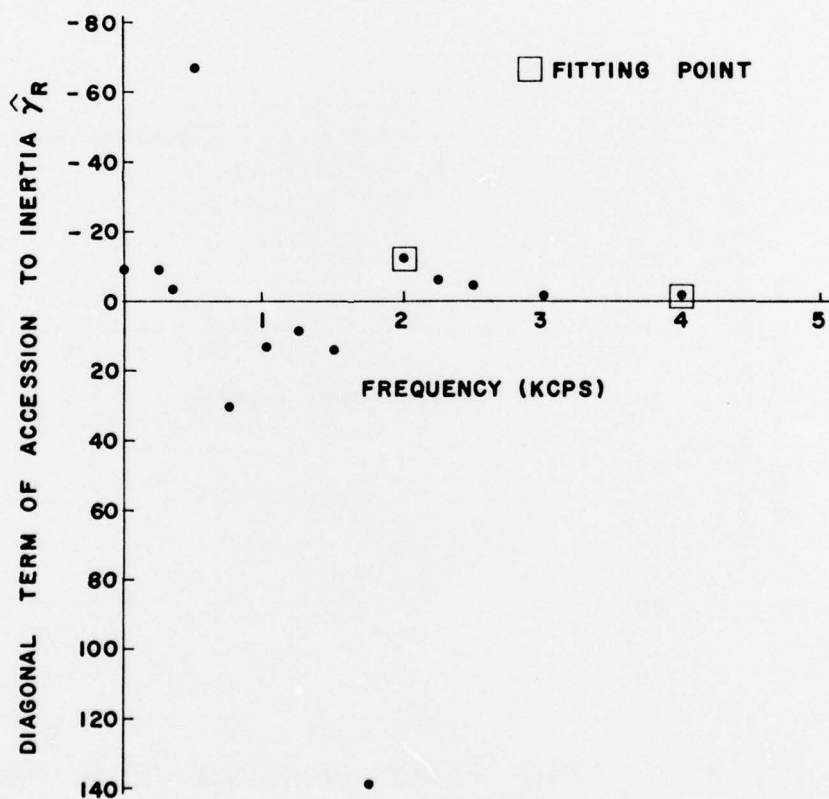


FIG. 4 FITTED FLUID RESPONSE (REAL PART)
SURFACE EXPANSION FUNCTION 12, N=1

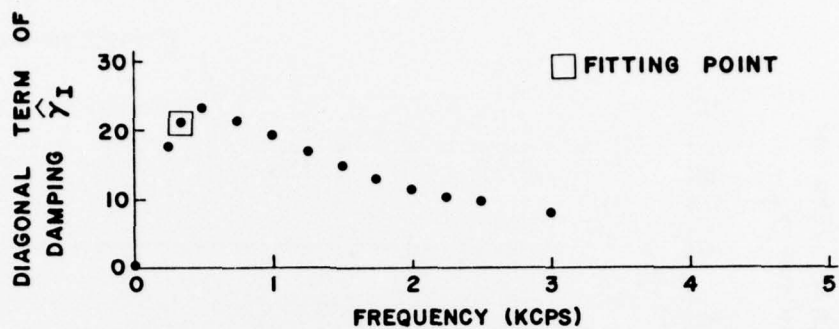


FIG. 5 FITTED FLUID RESPONSE (IMAGINARY PART)
SURFACE EXPANSION FUNCTION 1, N=1

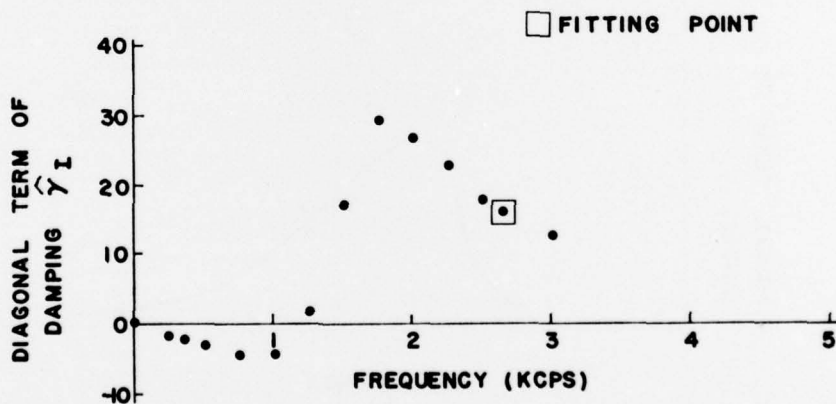


FIG. 6 FITTED FLUID RESPONSE (IMAGINARY PART)
SURFACE EXPANSION FUNCTION 12, N=1

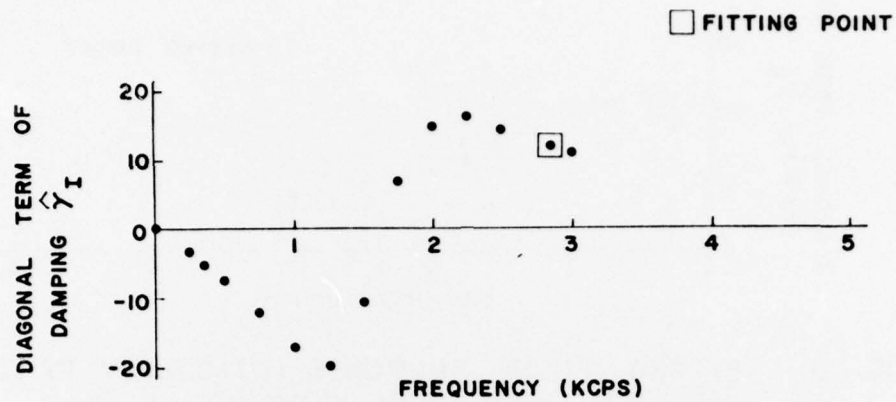


FIG. 7 FITTED FLUID RESPONSE (IMAGINARY PART)
SURFACE EXPANSION FUNCTION 13, N=1

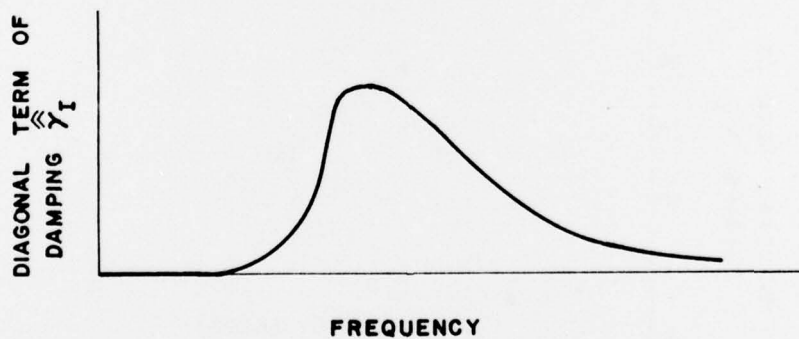


FIG. 8 TYPICAL BEHAVIOR OF A MAIN DIAGONAL TERM
OF DAMPING MATRIX

APPENDIX

Determination of Surface Expansion Functions which Diagonalize the Damping Matrix for High Frequencies and the Inertia Matrix for Low Frequencies.

In Ref. [2], elements of inertia and damping matrices, when surface expansion functions are used, are defined, respectively, as ^{*)}

$$\hat{\gamma}_{kj} = \int_A \hat{p}_j(s) \psi_k(s) dA \quad (A-1)$$

and

$$\hat{\bar{\gamma}}_{kj} = \int_A \hat{\bar{p}}_j(s) \psi_k(s) dA \quad (A-2)$$

In Eqs. (A-1) and (A-2), the ψ_k are the surface expansion functions. The \hat{p}_j and $\hat{\bar{p}}_j$ are defined by equations analogous to Eqs. (96) and (97) of Ref. [2]. In Eq. (95) of Ref. [2], the normal components of the shell modes, ϕ_j^n , are replaced by the ψ_j , and the generalized coordinates, \hat{q}_j , of Eq. (123) of Ref. [2] replace the q_j of Eq. (39) of Ref. [2].

The inertial and damping components of the generalized forces corresponding to the coordinates \hat{q}_j , defined by Eq. (126) of Ref. [2], are given by expressions analogous to Eqs. (110) and (98) of Ref. [2]:

$$\hat{Q}_{1k} = \sum_j \hat{\gamma}_{kj} \hat{q}_j \quad (A-3)$$

$$\hat{Q}_{2k} = \sum_j \hat{\bar{\gamma}}_{kj} \dot{\hat{q}}_j \quad (A-4)$$

^{*)} The elements of the inertia and damping matrices appearing in Eqs. (A-1) and (A-2) are related to the elements of the fluid resistance matrix of Section III by the expressions

$$\hat{\gamma}_{kj} = -\Omega_j^2 (\gamma_R)_{kj} \quad \text{and} \quad \hat{\bar{\gamma}}_{kj} = -\Omega_j (\gamma_I)_{kj}$$

where Ω_j denotes the frequency of the prescribed time-harmonic normal displacement. Details may be found in Ref. [2].

If the normalizing coefficients $\hat{\mu}_i$ of Eq. (124) of Ref. [2] are chosen equal to the shell surface area, the orthogonality condition becomes

$$\int_A \psi_i \psi_j dA = A \delta_{ij} \quad (A-5)$$

The choice of an orthogonal set of surface expansion functions is not unique. Given one set $\psi_i(s)$, new functions $\hat{\psi}_k(s)$ can be constructed as infinite series of these:

$$\hat{\psi}_k(s) = \sum_i r_i^{(k)} \psi_i(s) \quad (A-6)$$

Because the problem is linear, it follows from their definitions that the pressures $\hat{\hat{p}}_j(s)$ and $\hat{\bar{p}}_j(s)$ corresponding to the new set of surface expansion functions $\hat{\psi}_j(s)$ are related to the $\hat{p}_i(s)$ and $\bar{p}_i(s)$ obtained using $\psi_i(s)$ by relations similar to Eq. (A-6),

$$\hat{\hat{p}}_j(s) = \sum_i r_i^{(j)} \hat{p}_i(s) \quad (A-7)$$

$$\hat{\bar{p}}_j(s) = \sum_i r_i^{(j)} \bar{p}_i(s) \quad (A-8)$$

Using Eqs. (A-5) and (A-6), it follows that

$$\int_A \hat{\psi}_i \hat{\psi}_j dA = A \sum_m r_m^{(i)} r_m^{(j)} \quad (A-9)$$

Thus, if the $\hat{\psi}_j$ are also to be an orthogonal set in the sense of Eq. (A-5),

$$\sum_m r_m^{(i)} r_m^{(j)} = \delta_{ij} \quad (A-10)$$

As was shown in Section J of Ref. [2], the use of any set of orthogonal surface expansion functions leads to a diagonal damping matrix in the limit of infinite frequency, i.e.,

$$\lim_{\bar{\Omega} \rightarrow \infty} \hat{\bar{\gamma}}_{kj} = -\alpha_{kj} = -\rho c A \delta_{kj} \quad (A-11)$$

It is now desired to choose that (unique) orthogonal set of $\hat{\psi}_k$ [from among all those obtainable from Eq. (A-6) with coefficients satisfying Eq. (A-10)] which diagonalizes the inertia^{*)} matrix at zero frequency, i.e., which results in

$$\hat{\bar{\gamma}}_{kj} \Big|_{\bar{\Omega} = 0} = b^{(k)} \delta_{kj} \quad (A-12)$$

If Eqs. (A-6) and (A-7) are substituted into equations analogous to Eq. (A-1), with $\hat{\bar{\gamma}}_{kj}$ on the left-hand side instead of $\hat{\gamma}_{kj}$, there results

$$\hat{\bar{\gamma}}_{kj} = \sum_m \sum_n r_n^{(k)} r_m^{(j)} \hat{\gamma}_{nm} \quad (A-13)$$

Diagonalization at zero frequency is ensured by substituting Eq. (A-13) into Eq. (A-12):

$$\sum_m \sum_n r_n^{(k)} r_m^{(j)} \hat{\gamma}_{nm} \Big|_{\bar{\Omega} = 0} = b^{(k)} \delta_{jk} \quad (A-14)$$

Thus, the set (and only that set) of surface expansion functions which is obtained from Eq. (A-6) with expansion coefficients satisfying both Eqs. (A-10) and (A-14) will be orthogonal in the sense of Eq. (A-5) and produce diagonal damping and inertia matrices at infinite and zero frequencies, respectively, as expressed by Eqs. (A-11) and (A-12).

*) It should be noted that the elements of the inertia matrix, $\hat{\bar{\gamma}}_{kj}$, are related to those of the virtual mass matrix, $\hat{\gamma}_{kj}$, by

$$\lim_{\bar{\Omega} \rightarrow 0} -\hat{\bar{\gamma}}_{kj} / \bar{\Omega}^2 = \hat{\gamma}_{kj}$$

This may be seen by comparing the definitions of Eqs. (75) and (96) of Ref. [2] with surface expansion functions used instead of shell modes.

In partial matrix form, Eqs. (A-6), (A-10) and (A-14) may be written as

$$\hat{\psi}_i(s) = \underline{\psi}(s) \underline{r}^{(i)} \quad (A-15)$$

$$\underline{r}^{(i)} \underline{r}^{(j)} = \delta_{ij} \quad (A-16)$$

$$\underline{r}^{(i)} \hat{\underline{Y}}_{\underline{\Omega}} = 0 \quad \underline{r}^{(j)} = b^{(j)} \delta_{ij} \quad (A-17)$$

Equations (A-16) and (A-17) constitute a standard eigenvalue problem in which the elements of the (diagonal) inertia matrix at zero frequency, $b^{(j)}$, are the eigenvalues and the columns of expansion coefficients $\underline{r}^{(j)}$ are the corresponding eigenvectors. The solution of Eq. (A-17) which satisfies Eq. (A-16) is readily seen to be

$$(\hat{\underline{Y}}_{\underline{\Omega}} = 0 - b^{(j)} \underline{I}) \underline{r}^{(j)} = 0 \quad (A-18)$$

in which \underline{I} is a unit diagonal matrix. After the series of Eq. (A-6) is truncated by considering a finite number of expansion functions ψ_i , the eigenvalue problem of Eq. (A-18) may be solved by any standard method.